energy&fuels

Article

Cite This: Energy Fuels 2019, 33, 1256−1266

pubs.acs.org/EF

Release of Alkalis and Chlorine from Combustion of Waste Pinewood in a Fixed Bed

Xiaoxiao Meng,[†] Wei Zhou,*[,†] Emad Rokni,[‡] Guoyou Chen,[§] Rui Sun,*[,†] and Yiannis A. Levendis*[,‡]

[†]School of Energy Science and Engineering, Harbin Institute of Technology, Harbin 150001, P. R. China

[‡]Department of Mechanical and Industrial Engineering, Northeastern University, Boston, Massachusetts 02115, United States

[§]Agricultural Products Quality and Safety Research Institute, Heilongjiang Academy of Agricultural Sciences, Harbin 150001, P. R. China

ABSTRACT: Combustion of biomass in a boiler releases alkali metals and chlorine which, together with silicon and sulfur, are responsible for slagging, fouling, corrosion, and particulate emissions. This research investigated the effects of the primary (under-fire) air flow rate, $\dot{m}_{air}$, and its preheating temperature on the ignition and burning rates of pinewood chips in a laboratory fixed bed furnace and on the release of alkali metals and alkali earth metals (potassium (K), sodium (Na), calcium (Ca), magnesium (Mg)) and chlorine. The air flow rate, $\dot{m}_{air}$, through the bed was varied in the range of 0.085−0.237 kg/(m^2 s), resulting in an overall excess primary air coefficient λ varying from 0.56 to 1.1. Air was also preheated in the range of 20−135 °C. Results showed that increasing either $\dot{m}_{air}$ or the air preheat temperature increased the flame propagation rate (ignition rate) and the mass burning rate of the fuel. Moreover, the release of Cl was nearly complete (>99%) in all examined cases, whereas the release of alkalis was only partial. Calcium was the most predominant alkali in the pinewood; however, potassium was the predominant alkali in the released gases. The mass fraction of Na in the pinewood was much lower than that of K but it was released more comprehensively. Increasing the air flow rate enhanced the release of K and Na significantly, whereas it enhanced the release of Ca and Mg only slightly. Preheating the primary air preferentially increased the migration of K to the gas phase, whereas Na, Ca, and Mg were affected only mildly. The preheated air promoted the transfer of chlorine to HCl. Overall, moderately high primary air flow rates generate globally fuel lean conditions and mildly preheated air can enhance the mass burning rate of pinewood and its conversion to fully and partially oxidized gases. However, they result in enhanced gasification of the alkalis in the biomass. In the case of pinewood, this may be a minor concern, as the absolute values of such emissions are low relative to other biomass fuels.

1. INTRODUCTION

In recent years, concerns about the environmental consequences of the ever-increasing greenhouse gas emissions heightened the global interest in the development of renewable energy sources, such as biomass, solar, wind, tide, etc.[1−4] As a result, renewables are expected to be the fastest growing source of energy for electricity generation, with probably annual increases averaging 2.9% from 2012 to 2040.[5] Renewable biomass is a promising fuel because of low net CO_2 emissions and, thus, it can be used to substitute fossil fuels for heat and power generation.[4,6]

Combustion is a widely used technology for harvesting energy from biomass throughout humankind's history.[7] However, biomass generally contains a number of alkali and alkaline earth metals (AAEMs), Cl, Fe, S, etc., which can cause several issues, such as fouling, slagging, and corrosion of heat transfer surfaces, as well as particulate emissions.[8,9] These issues can have a detrimental effect on the operational efficiency and on the lifetime of combustion equipment.[10] Therein, potassium is typically the most important fouling species, and the nonmetallic element of Cl in those species (e.g., KCl) may accelerate corrosion of equipment during biomass thermochemical conversion.[11,12] Therefore, a better understanding of the release and transformation of AAEMs, particularly K, and Cl during biomass combustion can help address this particular technical problem caused by biomass utilization.

In addition, it is known that K is the most abundant cation in biomass for plant nutrition and growth etc., and as an important anion, Cl is responsible for balance;[13] both K and Cl ions are highly mobile. It has been reported that K transformations may occur during both devolatilization and char burnout stages, especially at high temperatures.[14−16] In addition, it is typically attested that the alkali metal K is either related to inorganic salts or it is organically bound to the carbonaceous matrix.[16−18] During the devolatilization stage, inorganic and organic K can transfer to each other; therein the release of K may be promoted as the organic matrix and can decompose even at low temperatures.[14,19]

Baxter et al.[8] burned woody and herbaceous materials in a biomass-fired boiler and reported that chlorine facilitates the mobility of many inorganic compounds, particularly potassium. Moreover, they concluded that the concentration of chlorine in biomass often dictates the amount of alkali metal vaporized during combustion more strongly than the concentration of alkali in the biomass. Biomass fuels with high potassium, chlorine, silicon, and sulfur contents, such as straws and other herbaceous plants, are particularly problematic as they cause furnace slagging and rapid fouling of heat transfer surfaces.[8] In

Received: November 15, 2018
Revised: December 20, 2018
Published: January 7, 2019

DOI: 10.1021/acs.energyfuels.8b03970
Energy Fuels 2019, 33, 1256−1266

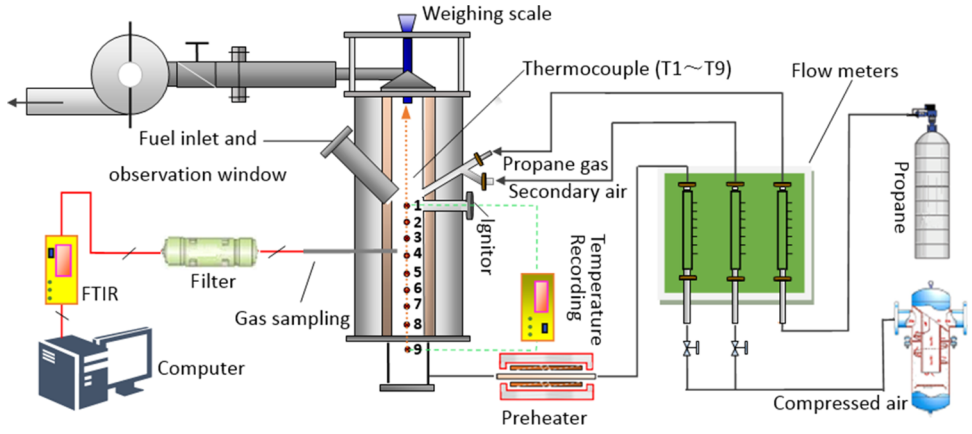

Figure 1. Schematic illustration of the fixed bed furnace for the combustion of the biomass fuels.

addition, the chlorides such as KCl and NaCl are known to increase the corrosion rate of stainless steel surfaces of superheater heat exchangers used inside boilers at temperatures lower than the melting temperature of the salts and their mixtures.[20] It was reposted that both KCl and NaCl are equally corrosive in the steam boilers, despite their different corrosive structures.[20] Therefore, during biomass combustion, attention should be paid to the emissions of alkali metals and HCl, which cause deposition on boiler surfaces, corrosion, and emit dust and incomplete combustion species, including CO and particulate matter.[21] All of these problems can disturb the combustion process, impair efficiency, and cause undesirable shutdowns. Furthermore, if HCl is released to the atmosphere, it can cause acid rain and respiratory diseases.[22−25] Also, HCl can be the precursor to dioxin formation in the presence of unburned carbon, as reported by Björkman and Strömberg.[13]

Previous work by Johansen et al.[26] investigated the release of Cl, S, and K during the combustion of wood chips and corn stover and observed that chlorine was nearly completely released, whereas K was only partially released. Meng et al.[27] burned various blends of pinewood (a low Cl, K, and S biomass) and corn straw (a high Cl, K, and S biomass) in a fixed bed and they also found that the release of chlorine was nearly complete. Moreover, they reported that the molar Cl/K ratio increased in the fuel blend as the amount of corn straw increased, resulting in enhanced alkali release to the gas phase, in agreement with the aforementioned conclusion of Baxter et al.[8] Ren et al.[4] addressed the emissions of hydrogen chloride from burning corn straw (a high Cl, K, and S biomass) in a fixed bed and found that chlorine was only partially released to the gas phase. Moreover, they found that increasing the flow rate of the primary air through the bed ($\dot{m}_{air}$) led to a higher conversion ratio of chlorine to hydrogen chloride. Finally, Meng et al.[28] burned a 50−50% blend of pinewood and corn straw (i.e., moderate Cl, K, and S blend) in a fixed bed and found that increasing $\dot{m}_{air}$ increased the amounts of both alkalis and chlorine released to the gas phase. This study focused on the important combustion performance parameters of waste pinewood chips (a low Cl, K, and S biomass) in a fixed bed and assessed the evolution of alkalis and chlorine. The effects of $\dot{m}_{air}$ through the bed and the effects of preheating air on the combustion performance parameters and the evolution of alkali and alkali earth metals (AAEMs) and chlorine (such as HCl) were investigated.

Woody biomass is most commonly used as fuel in grate combustors and, to a lesser extent, in fluidized bed furnaces. In the former combustors, moving grate systems are the prevalent equipment in medium and small-sized district heating and industrial units.[29−31] Fixed bed reactors with stationary grates can be used in the laboratory to simulate the moving grate systems.[31,32] This is because, compared to the prevalent vertical gradients of temperature and concentrations of species in the bed layer, the horizontal gradients are relatively small. Hence, heat and mass transfer in the bed can be only considered in the vertical direction.[33] A fixed bed reactor is simpler to operate and collect data with minimum running costs.[34] Therefore, this experimental study herein was performed in a fixed bed reactor with a stationary grate.

2. EXPERIMENTAL APPARATUS AND BIOMASS FUEL

2.1. Experimental Apparatus. Biomass was burned in a one-dimensional fixed bed inside a vertically oriented cylindrical combustion chamber, depicted in Figure 1. The chamber is 1.30 m high, with an inner diameter of 180 mm, and is composed of three layers of materials in the wall. The inner layer is made of 50 mm thick alumina refractory pouring, the middle insulating layer is composed of a 150 mm thick refractory fiber cotton wall, and the outer protective sleeve is made of $Cr_{18}Ni_9Ti$ steel. More details about the experimental test rig are given in ref 27.

The fixed bed furnace setup consists of four systems: the furnace, the air supply system, the air preheating system, and the measurement systems. During the experiments, heat was supplied to a fixed bed of biomass by burning propane gas. A gas nozzle was placed at a furnace height of 750 mm away from the grate and it was tilted to 45°. At the beginning of each experiment, a propane torch was ignited and then its flow rate was kept at a constant value that was sufficient to maintain the chamber temperature at around 900 °C. The pinewood was heated by radiation and convection from the high temperature propane flame. The bed temperatures were monitored by armored K-type thermocouples at different bed heights, at 11 different positions specified in Table 1. The measuring range of the armored K-type thermocouples was 0−1390 °C, with a measurement error of ±2.5 °C. A gas-sampling probe was inserted at 388 mm above the grate to monitor the gaseous emissions of combustion. In a number of experiments, the primary combustion air (under-fire air) was heated

Table 1. Thermocouple Locations in the Fixed Bed

number	distance to the grate surface (mm)	number	distance to the grate surface (mm)
1	748	6	208
2	560	7	118
3	478	8	28
4	388	9	−90
5	298		

DOI: 10.1021/acs.energyfuels.8b03970
Energy Fuels 2019, 33, 1256−1266

Table 2. Chemical Compositions (wt %) of the Selected Pinewood Fuel

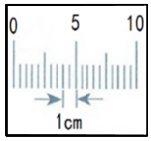	Value	Method	Reference
Ultimate analysis/wt%（dry basis）			GB/T 476-2001
Carbon (%)	47.65	Carbon dioxide absorption	
Hydrogen (%)	5.79	Water absorption	
Oxygen (%)	38.44	Calculation	
Nitrogen (%)	0.16	Pyrolysis and titration	
Sulfur (%)	0.02	Pyrolysis and coulometry	GB/T 214-1996
Chlorine (%)	0.017		
Calcium (%)	0.087		
Sodium (%)	0.008		
Potassium (%)	0.055		
Magnesium (%)	0.054		
Proximate analysis /wt%（dry basis）			GB/T 211-1996
Ash (%)	0.58	Slow ashing	
Moisture content (%)	4.72	Air drying	GB/T 212-2001
Fixed Carbon (%)	12.78	Calculation	GB/T 213-2003
Volatile matter (%)	81.80	Thermostatic firing	
Low Heating value (MJ/kg)	17.93	calorimeter	GB/T 213-2008

using an electric preheater incorporating a spiral-tube heat exchanger and, afterwards, it was supplied to the bottom wind box of the furnace and then to the fuel bed through the porous metal grate. Its flow was controlled by a flow meter and its temperature was monitored by the bottommost level 9 thermocouple (T9) shown in Figure 1.

2.2. Experimental Procedures and Fuel Properties. Air-dried pinewood was selected for these experiments based on its relatively high planting rate in northern China. Pinewood residues were collected from a timber mill of Heilongjiang Province, China. The proximate and ultimate analyses of air-dried pinewood (moisture content—4.72%) are listed in Table 2.

In these experiments, the pinewood chips were in the form of parallelepipeds with approximate dimensions of $5 \times 2 \times 1$ cm^3 and were packed in beds weighing approximately 2.5 kg and having heights of 540 mm and diameters of 180 mm. To investigate the effect of primary air flow on the AAEMs and Cl released to the gas phase during pinewood combustion, experiments were conducted with four different primary air flow rates through the grate at the bottom of the reactor (under-fire air) without preheating, i.e., at a temperature of 20 °C. The detailed experimental conditions are listed in Table 3. In addition, experiments were also conducted to preheat the primary air to the temperatures of 85 and 135 °C. On the basis of the stoichiometric fuel/air ratio of the pinewood fuel (approximated as $CH_{1.46}O_{0.61}N_{0.029}S_{0.0016}$ from its ultimate analysis) and on the actual fuel/air ratio from the experimental data, overall (global) excess air coefficients were calculated as $\lambda = (m_{air}/m_{fuel})_{actual}/(m_{air}/m_{fuel})_{stoichiometric} = (V_{air}A\Delta t\rho_{air}/m_{fuel})_{actual}/(m_{air}/m_{fuel})_{stoichiometric}$, ($\Delta t$ indicates the time of combustion and V_{air} is the air flow velocity and A represents the cross-sectional area of the bed) and are also shown in Table 3.

Table 3. Experimental Operating Conditions

primary air flow rate (L/min)	mass flux of primary air $\dot{m}_{air}$ (kg/(m^2 s))	excess primary air coefficient (λ)
100	0.085	0.56
160	0.135	0.87
230	0.194	0.92
280	0.237	1.1

The combustion effluent gases were first heated to 180 °C to avoid condensation of H_2O, which can absorb HCl and then they passed through a fiber filter to collect particles. Thereafter, gas analysis was performed by Fourier transform infrared spectroscopy (using a GASMET DX4000 instrument), which quantified HCl and other species, such as CO_2, CO, and CH_4, in the hot and humid sample gas. The LabVIEW software recorded the analyzer signals through a data acquisition card (Data Translation PCI-6221). All experiments were repeated in triplicates, the mean values of which and one standard deviation for each case are presented in the ensuing Experimental Results and Discussion Section.

During pinewood combustion, the bottom ash and the fly ash were also collected and analyzed by the following procedure. Solid ash samples were digested as a solution first, following the method in ref 4. (i) Solid particles were first dried at 105 °C for 2 h. (ii) Thereafter, the samples were added into an ultra-high purity (metal impurity content of less than 1 ppb) solution consisting of 6 mL of HNO_3 and 2 mL of H_2O_2 for 2 h. (iii) Subsequently, a new solution ($HNO_3/H_2O_2/HF$ = 4:2:2) was added into the samples and the samples were heated at a rate of 20 °C/min to 120 °C and were kept at this temperature for 5 min. (iv) Afterwards, the samples were heated at a heating rate of 16 °C/min to 200 °C and they were kept at this final temperature for 1 h. At the end of this procedure, the digested solutions were used to monitor (a) the mass fractions of AAEMs (Ca, K, Na, and Mg) in the ash by inductively coupled plasma atomic emission spectroscopy (ICP-AES) and (b) the

DOI: 10.1021/acs.energyfuels.8b03970
Energy Fuels 2019, 33, 1256−1266

Table 4. Mass Fractions of K, Na, Ca, Mg, and Cl in the Ash; Left Section: At No Air Preheat (T_{in} = 20 °C); Right Section: At a Fixed Air Flowrate ($\dot{m}_{air}$ = 0.135 kg/(m^{2}s))

	$\dot{m}_{air}$ (kg/(m^2 s))				preheated air temperature (°C)		
species	0.085	0.135	0.194	0.237	20	85	135
chlorine (%)	0.02	0.01	0.03	0.02	0.01	0.01	0.02
calcium (%)	24.11	25.51	26.91	28.41	25.51	25.99	26.59
sodium (%)	0.60	0.38	0.45	0.48	0.38	0.44	0.41
potassium (%)	5.59	5.68	5.39	5.08	5.68	5.49	4.58
magnesium (%)	6.12	7.06	7.01	7.09	7.06	6.76	6.82

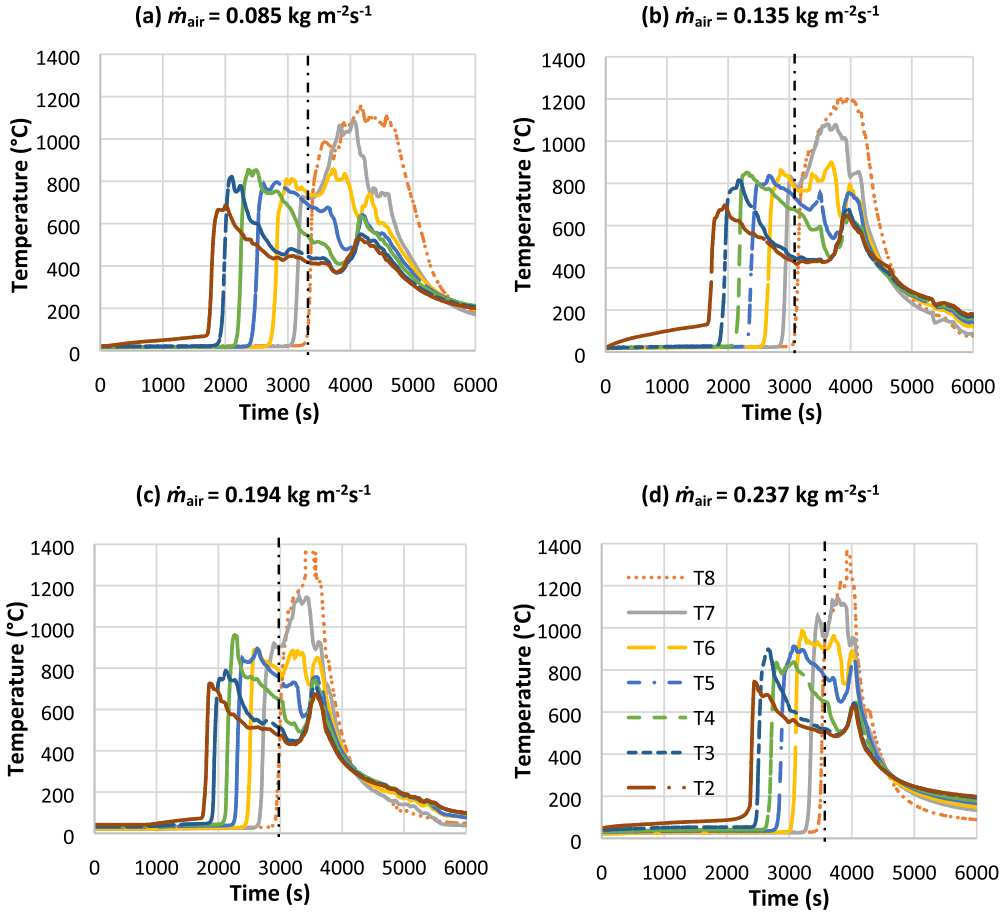

Figure 2. Bed temperature histories at different heights from the grate. The temperature of the primary air entering the bed was 20 °C. The vertical dashed lines denote that the flame approached the bottom of the bed and the char combustion became dominant near the grate surface.

mass fractions of Cl by ion chromatography. The corresponding fraction of AAEMs and Cl are listed in Table 4.

3. EXPERIMENTAL RESULTS AND DISCUSSION

3.1. Effects of Primary Air Flow Rate, $\dot{m}_{air}$, on AAEMs and Cl Release. *3.1.1. Combustion Characteristics.* The fuel bed temperature histories at different heights of the bed, which were monitored with the thermocouples T2−T8, are shown in Figure 2 at different $\dot{m}_{air}$ settings. The ignition delay, temperature gradient upon ignition (°C/s), the average flame propagation rate (ignition rate), and the average burning rate are listed in Table 5. The bed of pinewood chips was ignited at the top by a propane flame which heated the bed by radiation and convection, see Figure 1. The temperature gradient upon ignition was defined as the time elapsed for the temperature in each bed layer to increase from 300 to 800 °C.[35] Ignition delays were in the range of 1699−2370 s and were attributed to the times needed for heating up the fuel to its devolatilization temperature. Once the pinewood was ignited, at about 160 °C, the corresponding bed temperature increased rapidly as shown in Figure 2. With the increase of $\dot{m}_{air}$ in the range of 0.085−0.237 kg/(m^2 s), the temperature gradient increased from 7 to 11 °C/s (by ∼60%) because of the additional supply of oxygen (i.e., a higher λ).

Table 5. Combustion Parameters at Different Primary Air Flow Rates, $\dot{m}_{air}$

$\dot{m}_{air}$ (kg/(m^2 s))	0.085	0.135	0.194	0.237
ignition delay time (s)	1699	1705	1764	2370
temperature gradient (°C/s)	7	8	9	11
flame propagation rate (ignition rate) (mm/s)	0.33	0.38	0.45	0.47
burning rate (kg/(m^2 s))	0.025	0.027	0.034	0.035

After the flame front passed by the location of a given thermocouple, the bed temperature decreased mildly and then it leveled off. As hot combustion gases moved upwards, passing by the thermocouple, they experienced heat loss to the inner furnace walls, hence, their temperature dropped. At the same time, as the furnace walls got progressively hotter with time, the bed temperature at the location of that thermocouple increased again.[28,36] As the flame approached the

DOI: 10.1021/acs.energyfuels.8b03970
Energy Fuels 2019, 33, 1256−1266

bottom of the bed, the temperatures in layers (T7 and T8) were the hottest, exceeding by ~400 °C the temperatures of the upper bed layers; see Figure 2. This was attributed to diminished heat transfer, as the chamber wall heated up, and to widespread combustion of accumulated chars in addition to the combustion of any remaining volatiles. At increasingly higher $\dot{m}_{air}$, the peak temperatures of all layers increased and it even exceeded the upper limit of the K-type thermocouples used in these experiments. As a result, combustion became more intense and the fuel burnout time in each layer decreased.

Furthermore, with the increase of $\dot{m}_{air}$ the flame propagation rate (mm/s), which represents the flame travel velocity,[30] increased by ~40%. This parameter is also termed the ignition rate and represents the average propagation rate of an ignition wave.[35] Accordingly, the burning rate (kg/(m^2 s)), defined herein as the mass loss of the biomass over time per unit cross-sectional area of the cylindrical combustion chamber perpendicular to its vertical axis,[37] increased from 0.025 to 0.035 kg/(m^2 s), as listed in Table 5. Burning rates of pinewood are higher than those of corn straw examined earlier,[33] at comparable $\dot{m}_{air}$. The experimental burning rates are plotted against $\dot{m}_{air}$ in Figure 3.

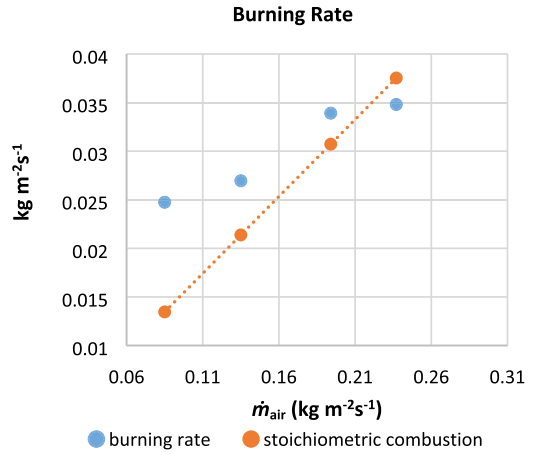

Figure 3. Actual and calculated stoichiometric burning rates of pinewood biomass as a function of $\dot{m}_{air}$.

Therein, calculated stoichiometric burning rates are also included. Actual burning rates are higher than stoichiometric burning rates at the first three experimental conditions, where the overall fuel-rich conditions prevailed. This difference may be attributed to the contributions of gasification reactions.[35] As the burning rates increased with $\dot{m}_{air}$, the amounts of unburned carbon remaining in the ashes on the grate, at the bottom of the bed decreased, from 12 to 4.5%, as shown in Table 6. This trend is in line with the increase of carbon conversion to CO_2 and CO with $\dot{m}_{air}$. Methane, was the most predominant detected unburned hydrocarbon and accounted for a significant fraction of the pinewood carbon, particularly so at the lower $\dot{m}_{air}$. This is in agreement with the aforementioned possibility of significant gasification reactions. Methane emissions decreased with increasing $\dot{m}_{air}$, such a phenomenon was attributed to the increased heat generation upon ignition and sufficient oxygen at higher $\dot{m}_{air}$.[3838] Therefore, it was confirmed that the combustion of the pinewood bed was more effective at high air flow rates.

3.1.2. Effect of $\dot{m}_{air}$ on AAEMs Release. The release of AAEMs (K, Ca, Na, and Mg) and chlorine to the gas phase during pinewood combustion in a fixed bed was calculated based on the difference of the initial contents of AAEMs and Cl in the raw pinewood, shown in Table 2, and their contents in the residual ashes after burnout,[29] shown in Table 4. Therefore, to investigate the release of K and other alkali metals during pinewood combustion, the mass-based emissions of AAEMs (mg/g fuel) are represented in Figure 4a, the molar emissions

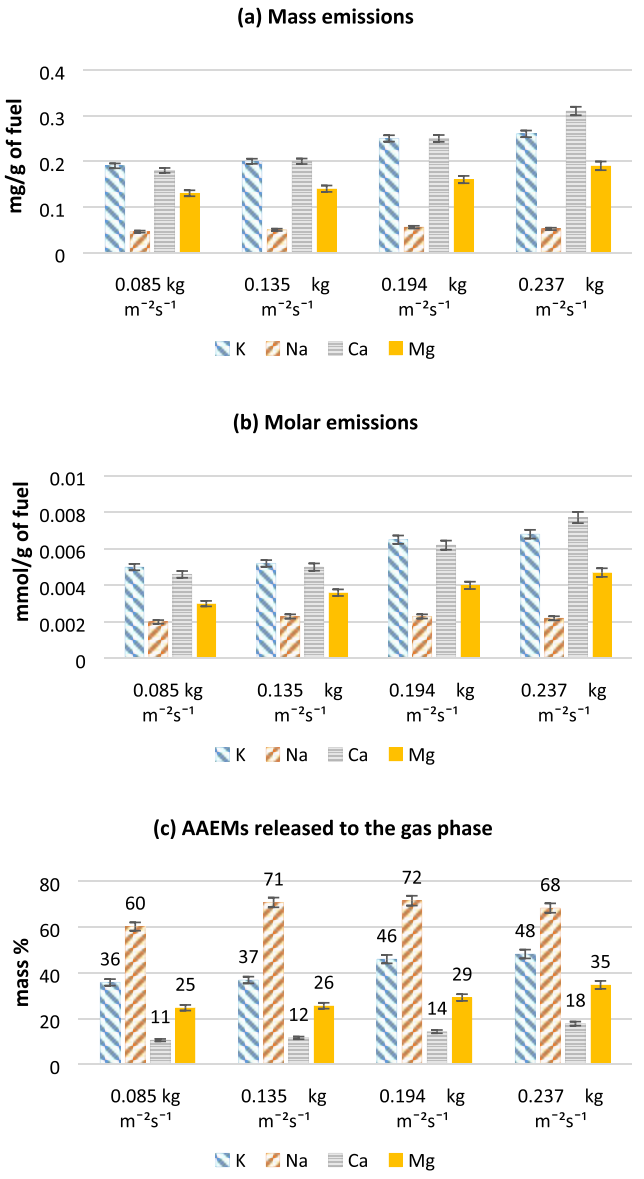

Figure 4. Integrated AAEMs (K, Na, Ca, and Mg) (a) mass emissions (mg/g pinewood), (b) molar emissions (mmol/g pinewood), and (c) mass fractions of AAEMs released to the gas phase during pinewood combustion in a fixed bed furnace. The temperature of the primary air entering the bed was 20 °C.

Table 6. Conversion of Carbon to Carbon-Containing Gases and Unburned Carbon in the Ash at Different Values of $\dot{m}_{air}$

$\dot{m}_{air}$ (kg/(m^2 s))	C (%) released as CO_2	C (%) released as CO	C (%) released as CH_4	C (%) released as C_2H_6	C (%) retained in the ash	C (%) not detected
0.085	42.7	9.3	12.6	0.12	12.0	23.27
0.135	44.1	12.9	10.9	0.08	7.3	24.7
0.194	50.6	16.3	10.0	0.07	5.5	17.6
0.237	57.2	20.0	6.5	0.09	4.5	11.8

DOI: 10.1021/acs.energyfuels.8b03970
Energy Fuels 2019, 33, 1256−1266

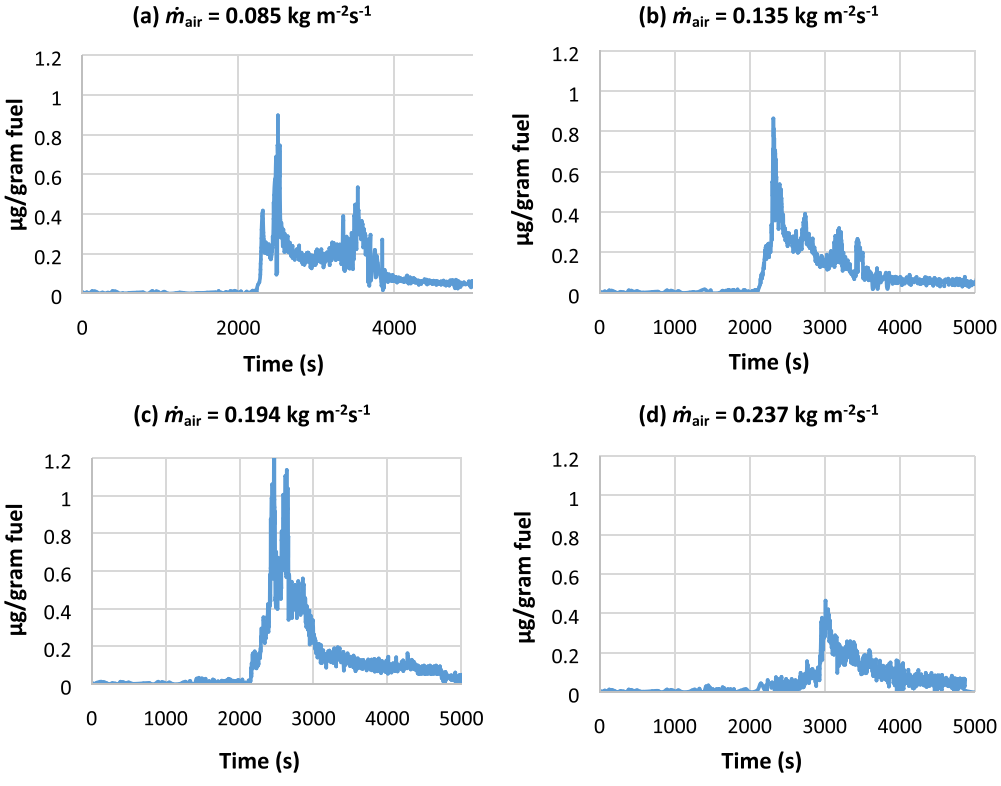

Figure 5. HCl mass emissions (μg/unit g pinewood) versus time at different air flow rates, $\dot{m}_{air}$. The temperature of the primary air entering the bed was 20 °C.

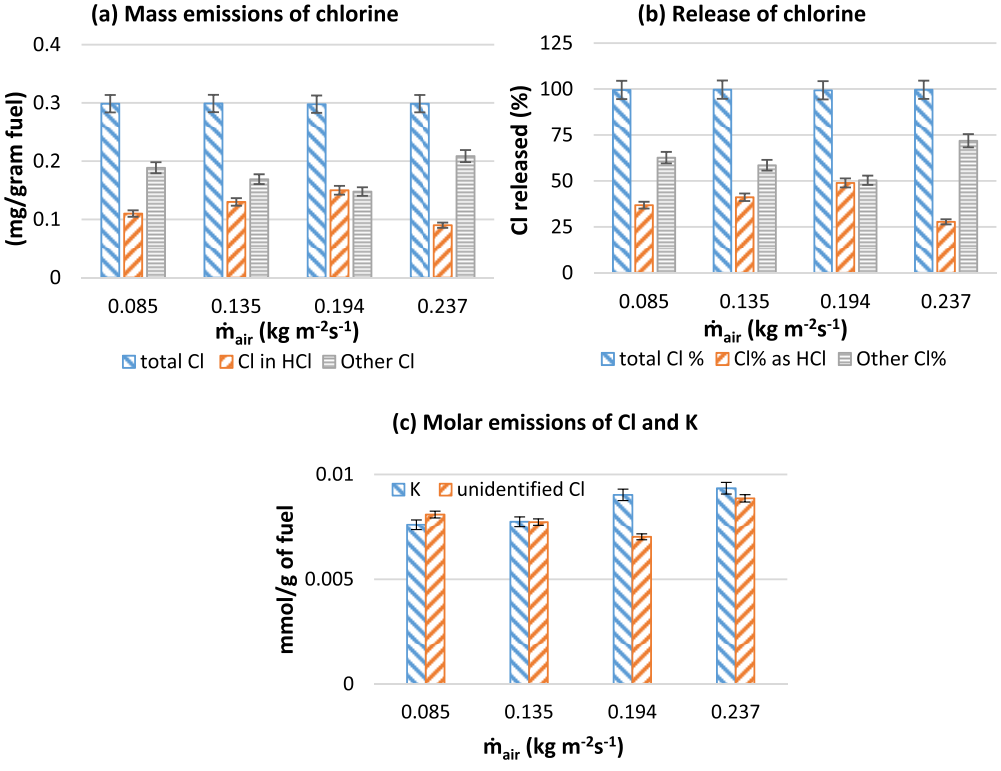

Figure 6. Integrated chlorine (a) mass emissions (mg/g pinewood); (b) fuel Cl (%) fraction released to the gas phase, Cl conversion to HCl, and Cl conversion to other gaseous species; (c) molar emissions (mmol/g pinewood) of K and Cl to the gas phase during pinewood combustion in a fixed bed furnace. The temperature of the primary air entering the bed was 20 °C.

(mmol/g fuel) are shown in Figure 4b, and the fractions of biomass AAEMs released to the gas phase are shown in Figure 4c. The results of this calculation show that calcium and potassium were the most prominent emissions of AAEMs followed by magnesium and sodium.

DOI: 10.1021/acs.energyfuels.8b03970
Energy Fuels 2019, 33, 1256−1266

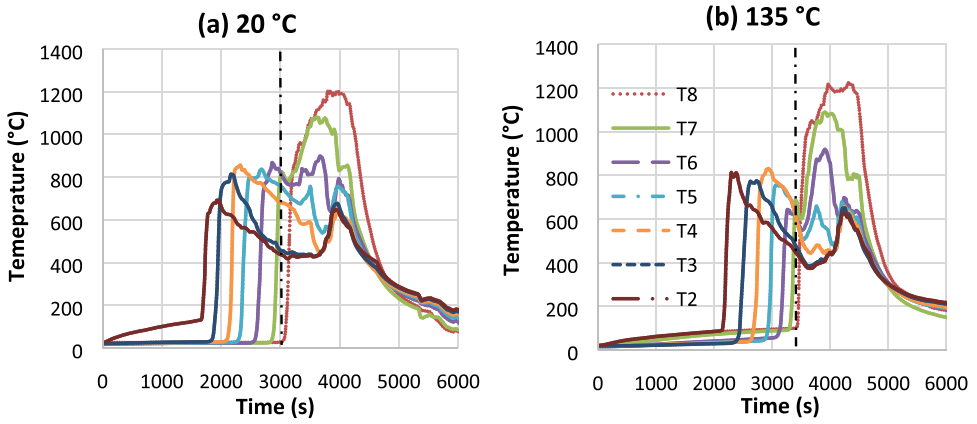

Figure 7. Bed temperature histories at different heights in the bed (typical air cases: (a) 20 °C without preheating air; (b) preheating air to 135 °C). The $\dot{m}_{air}$ was kept at 0.135 kg/(m^2 s). The vertical dashed lines denote that the flame approached the bottom of the bed and the char combustion became dominant near the grate surface.

The amounts of AAEMs released to the gas phase increased with increasing $\dot{m}_{air}$ as the bed temperatures got hotter; see Figure 2. Higher temperatures in the bed may have reached or exceeded the boiling points of K, Na and Mg, and Ca (759, 883, and 1070°, respectively) but barely that of Ca (1464° C).

The fractions of alkali earth metals (Ca and Mg) that were released to the gas phase were lower (10−19% and 24−34% respectively) than those of the alkali metals (K and Na which were 36−48 and 60−68%, respectively), whereas the mass emissions and molar emissions of Ca and Mg were higher than their aforementioned fractions; see Figure 4a,b. In addition, in the range of lower $\dot{m}_{air}$, 0.085−0.135 kg/(m^2 s), the variation of $\dot{m}_{air}$ had little effect on Ca release, which attests that Ca is stable in the solid particles. As reported by Aho et al.,[39] the main possible reaction pathway of Ca during the devolatilization stage is the reaction with sulfur oxide and the formation of stable $CaSO_4$, which can adhere to the surface of the solid particles. Therefore, increasing peak bed temperatures at higher $\dot{m}_{air}$, in the range of 0.294−0.237 kg/(m^2 s), exceeded the boiling point of Ca and caused an additional release (by 28%) to the gas phase. Furthermore, it has been reported[16,17] that during the char burning stage, escaping silicates to the outer structure of the biomass encounter the retained AAEMs and, upon preferential reaction with Ca and Mg, they remain in the ashes. This supports the observed low release of alkali earth metals to the gas phase during char combustion.

With the increase of $\dot{m}_{air}$, the fractions of K and Na released to the gas phase increased. Even if the fraction of sodium released was higher than the fraction of potassium, the total amount of the latter was higher than that of the former by a factor of five or more. This is because the pinewood contains nearly 10 times more K than Na; see Table 1. Since potassium is the most important fouling species in combustors,[40] the release and transformation of K during pinewood combustion is important. The increasing bed temperatures, with increasing $\dot{m}_{air}$, facilitate the release of K, both from inorganic salts and from organically bound compounds.[8−17] To assess the main form of K in the pinewood, chemical fractionation analysis was performed.[41] Powdered pinewood was mixed thoroughly with deionized water, and then the filtered fluid was tested for its K content by inductively coupled plasma atomic emission spectroscopy (ICP-AES). Based on the content of K element in the filtered fluid, it was determined that approx. 88.4% potassium could be dissolved in water; hence, it was concluded that most of K in pinewood was in the form of an inorganic salt. The results were consistent with those of Zhang et al.,[42] who reported that the main anions in pinewood water solution are Cl^- and HCO_3^-. Accordingly, the relatively lower melting point of potassium chloride (mp_{KCl} ~ 770 °C) than that of potassium carbonate ($mp_{K_2CO_3}$ ~ 900 °C)[43] suggests that KCl should be more volatile during the devolatilization stage. Therefore, the main release of K during the combustion of volatiles of pinewood was probably caused by the evaporation of KCl, which is in agreement with Zhang et al.[42] In fact, the bed temperature in the volatile burning stage did not reach the boiling point of KCl(s) (1420 °C). However, during the biomass devolatilization period ion-exchange reactions with function groups in the organic matrix, such as R-COOH(s) + KCl(s) → R-COOK(s) + HCl(g),[44] may have taken place. This is supported by the time-revolved evolution of HCl, shown in Figure 5. Most of the HCl appears to have been released during the volatile matter burning stage. During the char burning stage, with the increasing $\dot{m}_{air}$, the peak bed temperature increased to values reaching and exceeding 1400 °C. At these temperatures, K could be released to the gas phase, mostly as KCl and partially as K_2CO_3, etc. This is consistent with the results of Knudsen et al.[16]

3.1.3. Effect of $\dot{m}_{air}$ on Chlorine Release. The effect of $\dot{m}_{air}$ on the release of Cl was investigated in this work. As shown in Figure 6, the chlorine release from pinewood was nearly complete at all $\dot{m}_{air}$ conditions with the specific mass emissions of 0.3 mg/g fuel. This result is in contrast with the combustion of corn straw in this laboratory,[4] which released only 25−40% of its chlorine to the gas phase, albeit with much higher specific mass emissions in the order of 1−2 mg/g fuel, as pinewood has much lower chlorine and potassium contents than corn straw.[28] The fact that corn straw retains a higher fraction of its chlorine in the ash than pinewood can be explained based on the fact that it contains more organically bound chlorine, whereas such chlorine can be more readily released during the volatile phase and it can be recaptured by the alkalis in the char. Since corn straw has a high potassium content, far in excess of its chlorine content,[45] it can effectively capture more chlorine than pinewood in the chars. These results are in qualitative agreement with those of Johansen et al.,[26] who investigated the combustion of corn and wood blends in a grate reactor.

The fractions of Cl converted to HCl, shown in Figure 6, increased with the increase of $\dot{m}_{air}$, until 0.237 kg/(m^2 s) was reached and, thereafter, they decreased. Most of the HCl appeared to have been released during the volatile matter combustion stage; see Figure 5. The organic Cl can easily convert to HCl at a relatively low temperature (<500 °C) and up to 50 wt % of the Cl was released as HCl. At the same time, the release of other unidentified chlorine-containing species followed the opposite trend of HCl. Such species are likely to be mostly KCl, as previously mentioned, and in smaller amounts CH_3Cl and other alkali salts and carbonates. The likelihood that K is mainly released as KCl is supported by the fact that the molar emissions of K were nearly equivalent to those of Cl, as shown in Figure 6c. In addition, HCl emitted at the volatile combustion stage could be recaptured by K^+ in the char, since HCl-containing combustion gases moved upwards in the bed through the accumulating thick layer of chars, which moved downwards. The overall reaction can be represented as char-O−K^+(s) + HCl(g) → char-OH(s) + KCl(s,l).[46] As the maximum temperatures occurred at the char burning stage (near the bottom of the bed), see Figure 2, evaporation of KCl on the char occurred to the gas phase. Hence, higher K emissions occurred at higher $\dot{m}_{air}$, which induced higher char temperatures, see Figure 2. Moreover, the less stable K_2CO_3

DOI: 10.1021/acs.energyfuels.8b03970
Energy Fuels 2019, 33, 1256−1266

could have reacted with HCl, according to the K_2CO_3 + HCl(g) → 2KCl(g) + H_2O(g) + CO_2(g) reaction, which could have captured additional HCl and released more KCl.[46] However, with the increase of $\dot{m}_{air}$, the increasing CO_2 partial pressure (shown in Table 5) could have shifted the equilibrium to the opposite direction.[47]

It is possible that CH_3Cl could also have formed during biomass pyrolysis and combustion along with HCl.[48,49] CH_3Cl and HCl are competing for Cl radicals during biomass pyrolysis and combustion. It has been reported that Cl radical-generated CH_3Cl accounts for about 3% of the total chlorine-bearing gases during combustion[50,51] or even less at high temperatures.[4]

3.2. Effect of Preheated Air Temperature on AAEMs and Cl Release. The second part of this work investigated the effects of preheating the primary (over-fire) air temperature on the release of AAEMs and Cl during pinewood combustion in the fixed bed. In these experiments, the air flow rate was kept constant at 0.135 kg/(m^2 s). This particular flow rate was chosen because up to this value the release of K increased only mildly with $\dot{m}_{air}$, whereas beyond this value the release of K increased more drastically; see Figure 6c. Thus, higher flow rates were not chosen, as they might have obscured the investigation of the effects of preheated air on the release of AAEMs. As shown in Figure 7, increasing the air temperature from 20 to 135 °C, lengthened the ignition delay significantly (by 30%), and caused a shorter burnout time (by 18%). The experimental results confirmed that the biomass burns faster with preheated air, and the burning rate increased from 0.027 to 0.032 kg/(m^2 s) (by 18%) during pinewood combustion in a fixed bed, as shown in Table 7. This can be attributed to the fact that increasing the primary air temperature enhances moisture removal and, thus, the drying of the biomass.[52] Meanwhile, the flame propagation rate increased with the preheating of air, from 0.38 mm/s at 20 °C to 0.48 mm/s at 135 °C (by 26%). These results are in agreement with those of Zhao et al.,[36] who reported that the flame propagation rate is controlled by both the burning rate of the fuel and by the heat transfer to and from the flame zone.

Table 7. Combustion Parameters at Primary (under Fire) Air Preheat Temperatures at a Fixed Air Flowrate ($\dot{m}_{air}$ = 0.135 kg/(m^{2}s))

preheated primary air (°C)	20	85	135
ignition delay time (s)	1705	2180	2230
flame propagation rate or ignition rate (mm/s)	0.38	0.44	0.48
burning rate (kg/(m^2 s))	0.027	0.029	0.032

The combustion effectiveness of the fuel in the fixed bed was assessed based on the conversion of carbon in the fuel to CO_2 and/or the amount of unburned carbon in the ashes, shown in Figure 8. The CO_2 emission increased from 44 to 52% when the air preheat temperature increased from at 20 to 85 °C, the condition where the amounts of CO and unburned methane were the lowest. When air was preheated further to 135 °C, the CO_2 emissions decreased and those of CO and methane increased. The unburned carbon was lowest at the preheated air temperature of 85 °C. This observation suggests some irregularity of combustion in the bed, such as spot ignition away from the flame front. Therefore, better combustion effectiveness for the pinewood appeared to occur at a preheated air temperature of 85 °C.

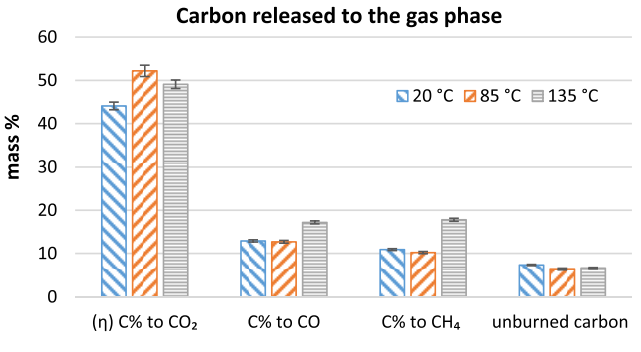

Figure 8. Conversion of C to CO_2, CO and CH_4, and unburned carbon during pinewood combustion at different preheated air temperatures. The $\dot{m}_{air}$ was kept at 0.135 kg/(m^2 s).

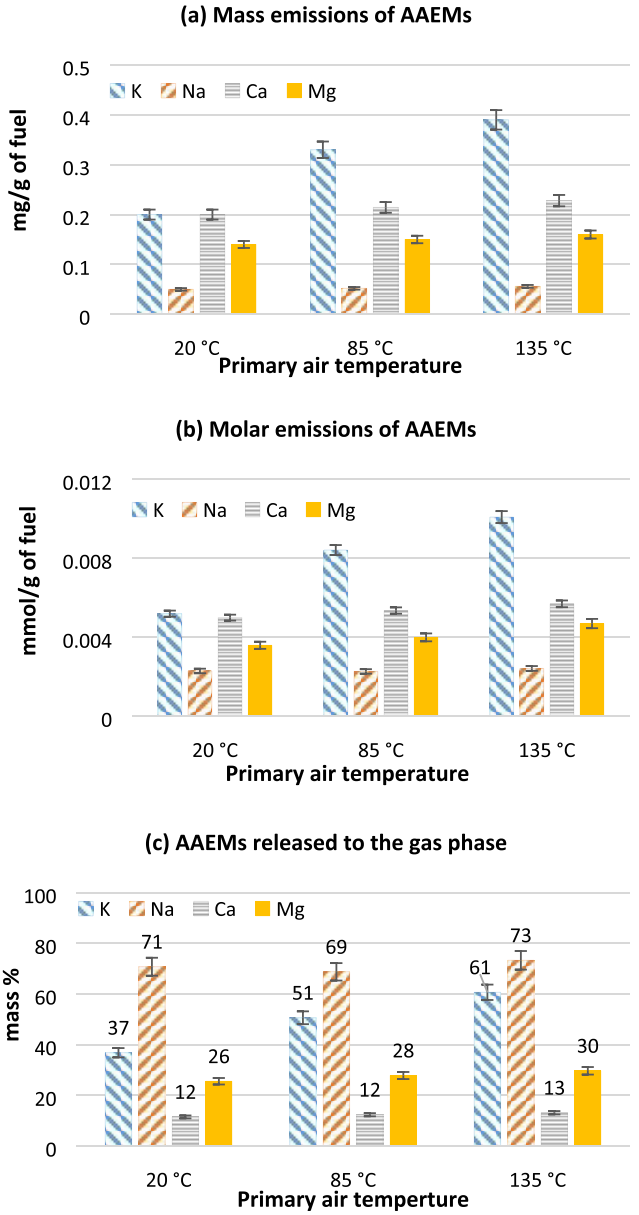

Figure 9. Integrated AAEMs (K, Na, Ca, and Mg) at different primary air temperatures: (a) mass emissions (mg/g pinewood), (b) molar emissions (mmol/g pinewood), and (c) mass fractions of AAEMs released to the gas phase during pinewood combustion in a fixed bed furnace. The $\dot{m}_{air}$ was kept at 0.135 kg/(m^2 s).

The mass amounts of AAEMs released to the gas phase increased with increasing the temperature of the preheated air, shown in Figure 9. Specifically, the emissions of K increased from 0.2 to 0.39 mg/g fuel, amounting to 37−61% of the potassium mass in the fuel as the temperature was increased from 20 to 135 °C. The corresponding sodium mass released to the gas phase was even higher, ranging from 69 to 73%, whereas those of calcium and magnesium were lower, ranging from 12 to 13% and from 26 to 30%, respectively. These results show that the temperature of the preheated air mostly affected the potassium release. At low temperatures, potassium exists in the char in the form of K-salts, mostly exposed on the surface of the solid particle. As the air

DOI: 10.1021/acs.energyfuels.8b03970
Energy Fuels 2019, 33, 1256−1266

temperature increased, higher flame temperatures were generated (see, for instance, T2 in Figure 7), which are likely to have enhanced the migration of K-salt to the gas phase. Moreover, it has been reported that increasing temperature leads to fuel particles with increased porosity,[16] which may have aided the migration of K-salt to the particle surface, and therefrom to the gas phase.

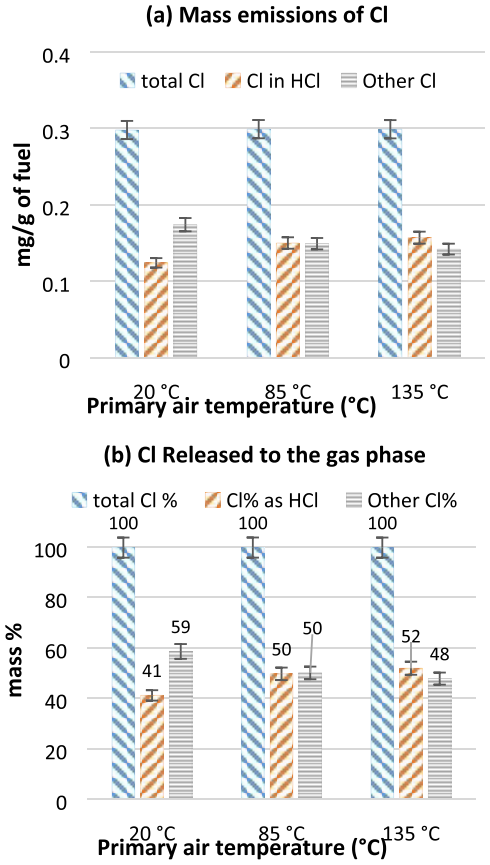

Figure 10. (a) Mass emissions of Cl (mg/g pinewood) and (b) release of fuel Cl (%) to the gas phase, conversion of fuel Cl to HCl, and to other chlorinated species during pinewood combustion in a fixed bed furnace. The $\dot{m}_{air}$ was kept at 0.135 kg/(m^2 s).

The amounts of fuel Cl released to the gas phase and the specific mass emissions of HCl, as well as those for other nonmeasured species are shown in Figure 10a, at different preheated air temperatures examined herein. The corresponding fractions of fuel Cl released to the gas phase as well as the fractions of fuel chlorine which were converted to HCl and to other unidentified species (such as KCl) are shown in Figure 10b. In all cases, the total Cl mass emissions were nearly 0.3 mg/g fuel, which corresponded to the entire mass of chlorine in the biomass, i.e., Cl was released in its entirety (100%), whether air was preheated or not. Meanwhile, by increasing the inlet air temperature from 20 to 135 °C, the mass emission of HCl increased from 0.124 to 0.157 mg/g fuel, with the corresponding fractions of Cl being converted to HCl increasing from 41 to 52%. The increased emissions of HCl may be attributed to the faster flame propagation rate and burning rate at higher air temperature. In addition, the preheated air accelerated the reaction rate of pinewood combustion at the volatile combustion stage.[53] This increase in HCl emissions may be attributed to the fact that high air preheat temperatures dried the fresh fuel in the bed. Then, as the generated steam moved upwards, it increased the temperature of the upper bed layers (seen in Figure 7) and it enhanced devolatilization which, in turn, promoted HCl release. This is supported by the findings of Yang et al.,[54] who reported that the increased moisture can produce higher flame temperatures. In such a case, the chemical equilibrium of the reaction $H_2O \rightleftharpoons OH + H$ is shifted to the products; therefore, the generated OH and H radicals can readily react with Cl radicals and augment the conversion of Cl to HCl at increasing preheat temperatures.

Besides HCl and KCl, other chlorinated species possibly released to the gas phase may include methyl chloride (CH_3Cl). Johansen[47] reported that CH_3Cl released from wood chips was less than 0.4% of the total quantity of Cl. Therefore, methyl chloride is not significant for the Cl balance and KCl may be the primary compound in the "other" category in Figures 5 and 10.

CONCLUSIONS

This investigation studied the effect of the specific primary (under-fire) air flow rate, $\dot{m}_{air}$, in a fixed bed and its degree of preheating on pinewood combustion performance parameters. The release of fuel-bound AAEMs and chlorine to the gas phase and the evolution of HCl were also investigated. Results from this laboratory-scale investigation revealed the following:

(a) Increasing the $\dot{m}_{air}$ from 0.085 to 0.237 kg/(m^2 s) increased the flame temperature, the flame propagation rate (ignition rate), and the burning rate of the fuel bed.
(b) Increasing the $\dot{m}_{air}$ increases the release of K to the gas phase significantly (from 35 to 48%) and also the release of Na significantly (from 60 to 72%). As the amount of K in the fuel was much higher than that of Na, the emitted K was more pronounced than the emitted Na by 5-fold.
(c) A large fraction (88%) of K in the pinewood fuel was found to be in the form of inorganic salts, which during combustion can generate gaseous KCl, and in lesser amounts K_2CO_3, particularly at high $\dot{m}_{air}$.
(d) The entirety of the Cl mass in the pinewood fuel was released to the gas phase at all combustion conditions examined. As the $\dot{m}_{air}$ increased, the amount of Cl converted to HCl increased from 38 to 49%, and then decreased to 27% at the highest flow rate.
(e) Preheating the primary air temperature from 20 to 135 °C increased the flame temperature, the flame propagation rate, and the burning rate, which resulted in increased volatilization of all of the alkalis, particularly K, the mass fraction of which increased from 35 to 61%.
(f) Preheating the primary air temperature from 20 to 135 °C promoted the HCl emission. The release of Cl as HCl increased from 41 to 52%.

Overall, a sufficiently high primary air flow rate resulting in an overall excess air coefficient bigger than unity ($\lambda > 1$) and a mild air preheat can be recommended to enhance the mass burning rate of pinewood and its conversion to fully- and partially oxidized gases (CO_2 and CO). However, such conditions result in enhanced gasification of the alkalis in the biomass. In the case of pinewood, which contains low mass fractions of Cl and AAEMs, the absolute values of such emissions are low relative to other biomass types, such as straw.

AUTHOR INFORMATION

Corresponding Authors

*(W.Z.). Tel.: (+86) 157-6553-2715. Fax: (+86) 0451-86412528. E-mail: zhouweidream@gmail.com.
*(R.S). Tel.: (+86) 139-0450-1168. Fax: (+86) 0451-86412528. E-mail: sunsr@hit.edu.cn.
*(Y.A.L). Tel.: (001) 617-373-3806. Fax: (001) 617-373-2921. E-mail: y.levendis@northeastern.edu.

ORCID

Rui Sun: 0000-0002-6542-2429

DOI: 10.1021/acs.energyfuels.8b03970
Energy Fuels 2019, 33, 1256−1266

Yiannis A. Levendis: 0000-0002-8158-2123

Notes

The authors declare no competing financial interest.

■ ACKNOWLEDGMENTS

This work has been supported by the Innovative Research Groups of the National Natural Science Foundation of China (Grant No. 51476046), the US National Science Foundation (Award No. 1810961), Harbin Institute of Technology and Northeastern University.

■ REFERENCES

(1) IEA. *World Energy Outlook 2016*; International Energy Agency: Paris, France, 2016, p 28.
(2) Tillman, D. A. Biomass Cofiring: The Technology, the Experience, the Combustion Consequences. *Biomass Bioenergy* **2000**, *19*, 365−384.
(3) Demirbas, A. Potential Applications of Renewable Energy Sources, Biomass Combustion Problems in Boiler Power Systems and Combustion Related Environmental Issues. *Prog. Energy Combust. Sci.* **2005**, *31*, 171−192.
(4) Ren, X.; Meng, X.; Panahi, A.; Rokni, E.; Sun, R.; Levendis, Y. A. Hydrogen Chloride Release From Combustion of Corn Straw in a Fixed Bed. *J. Energy Resour. Technol.* **2017**, *140*, No. 051801.
(5) OECD/IEA. *World Energy Outlook 2016*; International Energy Agency, 2016, pp 1−8.
(6) Gao, X.; Zhang, Y.; Li, B.; Xie, G.; Zhao, W. Experimental Investigation Into the Characteristics of Chars Obtained From Fast Pyrolysis of Different Biomass Fuels. *J. Energy Resour. Technol.* **2018**, *140*, 044501−5.
(7) Demirbaş, A. Biomass Resource Facilities and Biomass Conversion Processing for Fuels and Chemicals. *Energy Convers. Manage.* **2001**, *42*, 1357−1378.
(8) Baxter, L. L.; Miles, T. R.; Miles, T. R., Jr.; Jenkins, B. M.; Milne, T.; Dayton, D.; Bryers, R. W.; Oden, L. L. The Behavior of Inorganic Material in Biomass-Fired Power Boilers: Field and Laboratory Experiences. *Fuel Process. Technol.* **1998**, *54*, 47−78.
(9) Baxter, L. L. Ash Deposition during Biomass and Coal Combustion: A Mechanistic Approach. *Biomass Bioenergy* **1993**, *4*, 85−102.
(10) Romeo, L. M.; Gareta, R. Fouling Control in Biomass Boilers. *Biomass Bioenergy* **2009**, *33*, 854−861.
(11) Kassman, H.; Broström, M.; Berg, M.; Åmand, L. E. Measures to Reduce Chlorine in Deposits: Application in a Large-Scale Circulating Fluidised Bed Boiler Firing Biomass. *Fuel* **2011**, *90*, 1325−1334.
(12) Saidur, R.; Abdelaziz, E. A.; Demirbas, A.; Hossain, M. S.; Mekhilef, S. A Review on Biomass as a Fuel for Boilers. *Renewable Sustainable Energy Rev.* **2011**, *15*, 2262−2289.
(13) Björkman, E.; Strömberg, B. Release of Chlorine from Biomass at Pyrolysis and Gasification Conditions. *Energy Fuels* **1997**, *11*, 1026−1032.
(14) van Lith, S. C.; Jensen, P. A.; Frandsen, F. J.; Glarborg, P. Release to the Gas Phase of Inorganic Elements during Wood Combustion. Part 2: Influence of Fuel Composition. *Energy Fuels* **2008**, *22*, 1598−1609.
(15) Novaković, A.; Van Lith, S. C.; Frandsen, F. J.; Jensen, P. A.; Holgersen, L. B. Release of Potassium from the Systems K-Ca-Si and K-Ca-P. *Energy Fuels* **2009**, *23*, 3423−3428.
(16) Knudsen, J. N.; Jensen, P. A.; Dam-Johansen, K. Transformation and Release to the Gas Phase of Cl, K, and S during Combustion of Annual Biomass. *Energy Fuels* **2004**, *18*, 1385−1399.
(17) Jensen, P. A.; Frandsen, F. J.; Dam-Johansen, K.; Sander, B. Experimental Investigation of the Transformation and Release to Gas Phase of Potassium and Chlorine during Straw Pyrolysis. *Energy Fuels* **2000**, *14*, 1280−1285.
(18) Jiang, L.; Hu, S.; Sun, L. s.; Su, S.; Xu, K.; He, L. m.; Xiang, J. Influence of Different Demineralization Treatments on Physicochemical Structure and Thermal Degradation of Biomass. *Bioresour. Technol.* **2013**, *146*, 254−260.
(19) Davidsson, K. O.; Stojkova, B. J.; Pettersson, J. B. C. Alkali Emission from Birchwood Particles during Rapid Pyrolysis. *Energy Fuels* **2002**, *16*, 1033−1039.
(20) Enestam, S.; Bankiewicz, D.; Tuiremo, J.; Mäkelä, K.; Hupa, M.; et al. Are NaCl and KCl Equally Corrosive on Superheater Materials of Steam Boilers. *Energy Fuels* **2011**, *25*, 1396−1404.
(21) Tissari, J.; Sippula, O.; Kouki, J.; Vuorio, K.; Jokiniemi, J. Fine Particle and Gas Emissions from the Combustion of Agricultural Fuels Fired in a 20 KW Burner. *Energy Fuels* **2008**, *22*, 2033−2042.
(22) Nielsen, H. P.; Frandsen, F. J.; Dam-Johansen, K.; Baxter, L. L. Implications of Chlorine-Associated Corrosion on the Operation of Biomass-Fired Boilers. *Prog. Energy Combust. Sci.* **2000**, *26*, 283−298.
(23) van Loo, S.; Koppejan, J. *The Handbook of Biomass Combustion and Co-firing*; Earthscan, 2008; Vol. *1*.
(24) Mitchell, E. J. S.; Lea-Langton, A. R.; Jones, J. M.; Williams, A.; Layden, P.; Johnson, R. The Impact of Fuel Properties on the Emissions from the Combustion of Biomass and Other Solid Fuels in a Fixed Bed Domestic Stove. *Fuel Process. Technol.* **2016**, *142*, 115−123.
(25) Obernberger, I.; Brunner, T.; Bärnthaler, G. Chemical Properties of Solid Biofuels-Significance and Impact. *Biomass Bioenergy* **2006**, *30*, 973−982.
(26) Johansen, J. M.; Aho, M.; Paakkinen, K.; Taipale, R.; Egsgaard, H.; Jakobsen, J. G.; Frandsen, F. J.; Glarborg, P. Release of K, Cl, and S during combustion and co-combustion with wood of high-chlorine biomass in bench and pilot scale fuel beds. *Prog. Energy Combust. Sci.* **2013**, *34*, 2363−2372.
(27) Meng, X.; Sun, R.; Zhou, W.; Liu, X.; Yan, Y.; Ren, X. Effects of Corn Ratio with Pine on Biomass Co-Combustion Characteristics in a Fixed Bed. *Appl. Therm. Eng.* **2018**, *142*, 30−42.
(28) Meng, X.; Zhou, W.; Rokni, E.; Zhao, H.; Sun, R.; Levendis, Y. A. Effects of Air Flowrate on the Combustion and Emissions of Blended Corn Straw and Pinewood Wastes. *J. Energy Resour. Technol.* **2018**, No. 042205.
(29) Mandø, M. *Biomass Combustion Science, Technology and Engineering*; Woodhead Publishing, 2013; pp 61−83.
(30) Khodaei, H.; Al-Abdeli, Y. M.; Guzzomi, F.; Yeoh, G. H. An Overview of Processes and Considerations in the Modelling of Fixed-Bed Biomass Combustion. *Energy* **2015**, *88*, 946−972.
(31) Yang, Y. B.; Ryu, C.; Khor, A.; Sharifi, V. N.; Swithenbank, J. Fuel Size Effect on Pinewood Combustion in a Packed Bed. *Fuel* **2005**, *84*, 2026−2038.
(32) Saastamoinen, J. J.; Taipale, R.; Horttanainen, M.; Sarkomaa, P. Propagation of the Ignition Front in Beds of Wood Particles. *Combust. Flame* **2000**, *123*, 214−226.
(33) Liang, L.; Sun, R.; Fei, J.; Wu, S.; Liu, X.; Dai, K.; Yao, N. Experimental Study on Effects of Moisture Content on Combustion Characteristics of Simulated Municipal Solid Wastes in a Fixed Bed. *Bioresour. Technol.* **2008**, *99*, 7238−7246.
(34) Yin, C.; Rosendahl, L. A.; Kær, S. K. Grate-Firing of Biomass for Heat and Power Production. *Prog. Energy Combust. Sci.* **2008**, *34*, 725−754.
(35) Rogers, J. E. L.; Sarofim, A. F.; Howard, J. B.; Williams, G. C.; Fine, D. H. Combustion Characteristics of Simulated and Shredded Refuse. *Symp. (Int.) Combust.* **1975**, *15*, 1137−1148.
(36) Zhao, W.; Li, Z.; Wang, D.; Zhu, Q.; Sun, R.; Meng, B.; Zhao, G. Combustion Characteristics of Different Parts of Corn Straw and NO Formation in a Fixed Bed. *Bioresour. Technol.* **2008**, *99*, 2956−2963.
(37) Ryu, C.; Phan, A. N.; Yang, Y. B.; Sharifi, V. N.; Swithenbank, J. Ignition and Burning Rates of Segregated Waste Combustion in Packed Beds. *Waste Manage.* **2007**, *27*, 802−810.
(38) Brennan, L.; Owende, P. Biofuels from Microalgae-A Review of Technologies for Production, Processing, and Extractions of Biofuels and Co-Products. *Renewable Sustainable Energy Rev.* **2010**, *14*, 557−577.
(39) Aho, M.; Paakkinen, K.; Taipale, R. Destruction of alkali chlorides using sulphur and ferric sulphate during grate combustion of corn stover and wood chip blends. *Fuel* **2013**, *103*, 562−569.

DOI: 10.1021/acs.energyfuels.8b03970
Energy Fuels 2019, 33, 1256−1266

(40) Jenkins, B. M.; Baxter, L. L.; Miles, T. R.; Miles, T. R. Combustion Properties of Biomass. *Fuel Process. Technol.* **1998**, *54*, 17−46.
(41) Meng, X.; Sun, R.; Yuan, H.; Zhou, W.; Ren, X.; Zhang, R. Effect of Different Pyrolysis Temperature on Alkali Metal K and Na Emission and Existence in Semi-Char. *J. Chem. Ind. Eng.* **2016**, 0438−1157.
(42) Zhang, Z.; Song, Q.; Alwahabi, Z. T.; Yao, Q.; Nathan, G. J. Temporal Release of Potassium from Pinewood Particles during Combustion. *Combust. Flame* **2015**, *162*, 496−505.
(43) Lehman, R. L.; Gentry, J. S.; Glumac, N. G. Thermal Stability of Potassium Carbonate near Its Melting Point. *Thermochim. Acta* **1998**, *316*, 1−9.
(44) Frandsen, F. J.; van Lith, S. C.; Korbee, R.; Yrjas, P.; Backman, R.; Obernberger, I.; Brunner, T.; Jöller, M. Quantification of the Release of Inorganic Elements from Biofuels. *Fuel Process. Technol.* **2007**, *88*, 1118−1128.
(45) Ren, X.; Sun, R.; Meng, X.; Vorobiev, N.; Schiemann, M.; Levendis, Y. A. Carbon, Sulfur and Nitrogen Oxide Emissions from Combustion of Pulverized Raw and Torrefied Biomass. *Fuel* **2017**, *188*, 310−323.
(46) Knudsen, J. N.; Jensen, P. A.; Lin, W.; Dam-Johansen, K.; et al. Secondary Capture of Chlorine and Sulfur during Thermal Conversion of Biomass. *Energy Fuels* **2005**, *18*, 810−819.
(47) Johansen, J. M.; Jakobsen, J. G.; Frandsen, F. J.; Glarborg, P. Release of K, Cl, and S during Pyrolysis and Combustion of High-Chlorine Biomass. *Energy Fuels* **2011**, *25*, 4961−4971.
(48) Eklund, G.; Pedersen, J. R.; Strömberg, B. Methane, Hydrogen Chloride and Oxygen Form a Wide Range of Chlorinated Organic Species in the Temperature Range 400 °C-950 °C. *Chemosphere* **1987**, *16*, 161−166.
(49) Palmer, T. Y. Combustion Sources of Atmospheric Chlorine. *Nature* **1976**, *263*, 44−46.
(50) Andreae, M. O.; Atlas, E. L.; Harris, G. W.; Helas, G.; DeKock, A.; Koppmann, R.; Maenhaut, W.; Mano, S.; Pollock, W. H.; Rudolph, J.; Scharffe, D. H.; Schebeske, G.; Welling, M. Methyl Halide Emissions from Savanna Fires in Southern Africa. *J. Geophys. Res.: Atmos.* **1996**, *101*, 23603−23613.
(51) Lobert, J. M.; Keene, W. C.; Logan, J. A.; Yevich, R. Global Chlorine Emissions from Biomass Burning: Reactive Chlorine Emissions Inventory. *J. Geophys. Res.: Atmos.* **1999**, *104*, 8373−8389.
(52) Warnecke, R. Gasification of Biomass: Comparison of Fixed Bed and Fluidized Bed Gasifier. *Biomass Bioenergy* **2000**, *18*, 489−497.
(53) Liang, L. Experimental Study and Numerical Simulation on Combustion Characteristics of Simulated Municipal Solid Wastes in a Fixed Bed. Ph.D. Thesis; Harbin Institute of Technology, 2008.
(54) Yang, Y. B.; Sharifi, V. N.; Swithenbank, J. Effect of Air Flow Rate and Fuel Moisture on the Burning Behaviours of Biomass and Simulated Municipal Solid Wastes in Packed Beds. *Fuel* **2004**, *83*, 1553−1562.

DOI: 10.1021/acs.energyfuels.8b03970
Energy Fuels 2019, 33, 1256−1266